Lawrence Berkeley Laboratory
UNIVERSITY OF CALIFORNIA

Materials & Molecular
Research Division

Submitted to Physical Review A

THE VALENCE PHOTOELECTRON SATELLITES OF NEON

P.A. Heimann, C.M. Truesdale, H.G. Kerkhoff,
D.W. Lindle, T.A. Ferrett, C.C. Bahr,
W.D. Brewer, U. Becker, and D.A. Shirley

November 1984

Prepared for the U.S. Department of Energy under Contract DE-AC03-76SF00098

DISCLAIMER

LBL-18263

The Valence Photoelectron Satellites of Neon

P.A. Heimann, C.M. Truesdale,* H.G. Kerkhoff,† D.W. Lindle,
T.A. Ferrett, C.C. Bahr, W.D. Brewer,‡ U. Becker,† and D.A. Shirley

Materials and Molecular Research Division
Lawrence Berkeley Laboratory
and
Department of Chemistry
University of California
Berkeley, California 94720

Abstract

Synchrotron radiation was directed at neon gas, creating Ne^+ ions in "satellite" states characterized by the configurations $1s^2 2s^2 2p^4 nl$, in addition to the main line final states: $2s^{-1}$ and $2p^{-1}$. Satellite features appearing in the photoelectron spectrum were studied in the near-threshold region with photon energies from 55.2 to 99.7 eV. For three of the satellite peaks, the angular distribution asymmetry parameter, β_i, varies with kinetic energy in much the same way as the asymmetry parameter of the 2p line. None of the satellites have a β_i like that of the 2s line. All the satellite partial cross sections, σ_i, have a kinetic energy dependence similar to the partial cross section of the 2p main line. However, the σ_i curves are not identical, and some deviation from the 2p intensity behavior is observed. These β_i and σ_i results are used to confirm the previous assignments of the satellite final states in neon and to consider, in general, the energy-dependent behavior of

satellites near threshold.

---

*Research and Development Division, Corning Glass Works, Corning, NY 14831
†Fachbereich Physik, Technische Universität Berlin, 1000 Berlin 12, W. Germany
‡Institut fur Atom und Festkorperphysik, Fachbereich Physik, Freie Universität Berlin, Arnimallee 14, 1 Berlin 33, W. Germany

I. Introduction

In simple systems such as atomic neon, the photoelectron spectrum is dominated by intense peaks associated with the removal of a single electron from the nominal ground-state configuration of the parent atom; e.g.,

$$Ne(1s^2 2s^2 2p^6;\ ^1S) \rightarrow Ne^+(1s^2 2s^2 2p^5;\ ^2P_{1/2,3/2}) + e^- \ .$$

These "main" peaks are analogous to the "diagram" lines in x-ray spectra.

Also present, usually with much lower intensity, are "satellite" peaks, which fall at higher binding energies than the main peaks. For heuristic reasons these satellites have been called "shake-up" peaks, because their dominant configurations could be accessed in a hypothetical two-electron excitation process; e.g.,

$$Ne(1s^2 2s^2 2p^6) + h\nu \rightarrow e^- + Ne^+(1s^2 2s^2 2p^4 n\ell) \ .$$

Here one 2p electron would undergo photoejection, and another would simultaneously be "shaken up" into the $n\ell$ orbital by the changing Coulomb field. In this approximation the satellite intensity can be estimated as being proportional to the square of the overlap matrix element between the passive electrons in the initial and final states; i.e., excluding the initial and final orbitals of the photoelectron.[1]

A more general theoretical approach takes electron correlation into account and employs multi-configuration wave functions in both

the initial and final states.[2] The satellite peaks are then associated with "correlation states," which are accessed by the same process that gives rise to the main peak. This approach restores the qualitative equivalence of the ionic "main" and "satellite" states and liberates the latter from their dependence on being created through the somewhat artificial "shake-up" process. Using a single configuration initial state and a multi-configuration final state, Dyall and Larkins[2,3] have calculated the binding energies and high energy intensities of the neon valence satellites.

These theoretical approaches have been adequate for providing an understanding of the existing satellite data measured with fixed-energy laboratory-based photon sources. The majority of correlation-satellite studies have been addressed to the energies of satellite peaks and to their intensities in the high energy (sudden) limit. A notable exception is an early paper on neon by Wuilleumier and Krause,[4] in which these authors used laboratory sources at several fixed energies to do pioneering studies of the kinetic energy (ϵ) dependence of satellite cross sections σ_i and angular distribution asymmetry parameters β_i. Wuilleumier and Krause noted that studies of $\sigma_i(\epsilon)$ and $\beta_i(\epsilon)$ should yield insights into the symmetry of the correlation satellite states and the mechanism by which they are populated. They also introduced the useful concept of the relative excitation energy, ϵ/E_0, where E_0 is the energy separating the correlation state from the main-line state. The ratio ϵ/E_0 can be regarded qualitatively as an adiabaticity parameter.[1]

With the availability of synchrotron radiation, there now exists the capability of controlling ϵ continuously. Of special interest is the possibility of making measurements of $\sigma_i(\epsilon)$ from the adiabatic regime, just above threshold, to the high ϵ sudden limit. Additional information can be gained by measuring $\beta_i(\epsilon)$ through the range of ϵ in which β of the main line exhibits its characteristic variation: in the neon case, near threshold, where β_{2p} varies greatly. In this paper we report a synchrotron-radiation study of the neon 2s, 2p satellites in which $\sigma_i(\epsilon)$ and $\beta_i(\epsilon)$ were measured through the range between ϵ = 3-6 eV and $\epsilon \sim 40$ eV (between ϵ/E_0 = 0.1-0.2 and $\epsilon/E_0 \sim 1.2$). Parallel experiments have examined the outer shell satellites of other atoms: He[5], Ar[6], and Xe.[7]

The experiment and data analysis are described in Section II. The spectral peak assignments are discussed in Section III. Section IV is devoted to the angular distribution results, and Section V to the partial cross sections. Finally, Section VI contains the conclusions.

II. Experimental

This experiment was performed at the Stanford Synchrotron Radiation Laboratory (SSRL) using a grazing incidence "grasshopper" monochromator with a 1200 line/mm grating. A 1000Å thick Si window isolated the monochromator vacuum from the experimental chamber. During the experiment the background pressure of the chamber was about 5×10^{-4} torr. We estimate that the pressure in the interaction

region was approximately a factor of 10 higher.

Photoelectrons were analyzed by the time delay between the synchrotron light pulse and the arrival of the electrons at one of two detectors. This method has been described elsewhere.[8,9]

The simultaneous measurement at two angles, $\theta = 0^\circ$ and 54.7°, yields the reported quantities $\beta_i(\varepsilon)$ and $\sigma_i(\varepsilon)$ from Yang's theorem:[10]

$$\frac{d\sigma_i(\varepsilon,\theta)}{d\Omega} = \frac{\sigma_i(\varepsilon)}{4\pi}\left[1 + \beta_i(\varepsilon)P_2(\cos\theta)\right] . \qquad (1)$$

Here the subscript i denotes a particular satellite peak, and θ is the angle between the photon electric vector and the photoelectron propagation direction. The dipole approximation, a randomly oriented sample, and linear polarized light have been assumed. The intensities measured provide branching ratios of the satellite peaks with respect to the 2s line, σ_i/σ_{2s}. All the intensity ratios presented here compare two transitions at the same photon energy. To obtain σ_i the satellite to 2s ratio was multiplied by σ_{2s} from Wuilleumier and Krause.[11]

For calibration, the transmission of the 54.7° analyzer and the relative efficiencies of the two analyzers were evaluated from the measured intensity of the 2s peak in combination with the literature cross section,[11] and the known value of $\beta_{2s} = 2$. The transmission function was corrected for changes in the light intensity, the percentage of higher-order light components, and the gas pressure.

To determine the peak areas and binding energies, the time-of-flight spectra (which were linear in time) were converted to a linear energy scale. Using a least-squares program, the satellite peaks were then fitted to Gaussian functions. Figure 1 displays the fit of a converted spectrum. The unresolved satellites 6 and 7 were fitted to 2 Gaussians separated by a fixed 0.55 eV, the approximate difference in binding energies. An exponential tail was combined with the Gaussian for the 2s peak, which was asymmetrically broad on the low kinetic energy side. For the background the sum of two functions was used: the first being constant in energy, and the second constant in time, varying as $\varepsilon^{-3/2}$. The binding energies were determined from the separation between the satellites and the 2s main line, which has a binding energy of 48.48 eV.[12,13]

The error bars provided for the $\sigma_i(\varepsilon)$ and $\beta_i(\varepsilon)$ data in this work represent either the standard deviations of the fits or the agreement between different spectra taken at the same photon energy. For the most important systematic error, that resulting from the calibration procedure, we estimate the uncertainty in β to be 0.1 and the uncertainty in the branching ratio to be 5 percent. At the lowest kinetic energies, 5 eV or less, the calibration error increases to about 0.15 in β and to 10-20 percent in the branching ratio.

III. The Energy Spectrum

The spectrum shown in Figure 1 was accumulated in 3000 sec with an accelerating voltage of 13 volts. The numbers labeling the

satellite peaks follow the notation of Wuilleumier and Krause[4] and will be used throughout this discussion. Our total experimental resolution can be seen, for example, in the observed width of the satellite peak 7, which is 0.41 eV FWHM. Convoluted in this width is the monochromator bandwidth, estimated to be 0.33 eV.

For the satellites appearing in this spectrum, Table 1 lists our binding energies along with the final ionic states as assigned by Dyall and Larkins[3] and with the energies from emission spectroscopy.[12] Wuilleumier and Krause identified several other peaks with very low intensity. With an improved signal-to-background ratio, we do not observe peaks 5, 8 (attributed by them to 2p electrons having undergone two inelastic collisions), 9, and 12. Dyall and Larkins could not find assignments for these features, either.

At photon energies above 66 eV, satellites 1 and 2 are observed. Because of their low intensity, only a brief description of their behavior will be given here. Satellite 1 has a β_i of 0.3(3) and a branching ratio with respect to the 2s main line of 2.3(3) percent, averaged over energy. For satellite 2, β_i increases from about 0 at 10 eV kinetic energy to about 1 at 35 eV. Similarly, the branching ratio of satellite 2 rises from approximately 1.5 to approximately 3 percent over the same energy range.

For two of the peaks appearing in Fig. 1, their shape implies some partly hidden structure. First, satellite 6 appears as a shoulder on the low kinetic energy side of satellite 7. In the 54.7° spectrum at 64.1 eV, satellite 6 is more prominent. Secondly,

satellite 3 is always unnaturally broad. Figure 2 displays the satellite peak widths from five similar spectra. The larger width of satellite 3 probably results from the summing of significant contributions from more than one of the final states listed in Table I. Comparison of the binding energy of satellite 3 with the energies of these final states suggests that one or more of the $(^1D)3d$ states should be an important component in this peak.

At this point some qualitative observations can be made about the satellite spectrum as a whole. First, all but the weakest lines can be assigned to configurations containing an excited orbital n with n=3. Therefore, processes leaving the Ne^+ ion with higher values of n seem to be less important. Secondly, final states of the form np $^2p^o$ are more important than those of the type ns ^2S or nd ^2S. In other words, satellites of the 2p main line are more important than those of the 2s line. This result, which will be confirmed in the following section by the β_i curves, is expected because the 2p channel is much more intense than the 2s in this energy range. In fact, the branching ratio σ_{2p}/σ_{2s} varies from 28 at 55 eV to 10 at 100 eV.[11] Having made separate calculations for the ^2S and $^2p^o$ manifolds, Dyall and Larkins assumed that the 2s and 2p satellites would be scaled by the main line branching ratio of the 2s and 2p cross sections. This argument implies that at high photon energy, i.e. 1 keV or more, satellites of the 2s peak should dominate over the 2p satellites. In Ar, Kr, and Xe a dissimilar situation exists because of the unusually strong interaction between the $nsnp^6$

and ns^2np^4nd configurations.[3]

IV. Angular Distributions

A complete assignment from the energy spectrum alone would require a degree of resolution unobtainable by the present or by earlier studies, and beyond the accuracy of theory. As seen in Table I, there are too many final states, too closely spaced. However, the angular distribution asymmetry parameters can provide additional information. Manson and Starace[14] applied the angular momentum transfer formalism to the term dependence of angular distributions. Assuming LS coupling, they showed that for certain transitions all final states with the same ^{2S+1}L must have identical β_i parameters. Applying these rules to Ne, the ^2S main line and satellite final states must have a β value of 2 independent of energy. Similarly, β_i is -1 for the ^2P states. These geometrical arguments do not restrict the β_i variation of the $^2P^o$ or ^2D states. However, the same algebraic expression in terms of scattering amplitudes applies to β_i of the 2p main line as well as the other $^2P^o$ transitions. While the scattering amplitudes need not be the same, the $^2P^o$ satellites should have β_i curves similar to that of the 2p main line.

Table II presents the numerical values of β_i, and Fig. 3 shows the β_i results as functions of kinetic energy for the five satellite peaks. Included in these plots are the β_i values obtained by Adam.[15] While confirming the observed trends for the three higher

binding energy satellites, Adam's β_i results are systematically higher than ours.

For three satellite peaks--4, 6+7, and 10--the observed β_i variation with energy is very much like β_{2p},[15] though for satellite 10, β_i seems to fall somewhat below the β_{2p} curve. In the case of satellites 4 and 10, the state assignments in Table I for these $^2P^o$ peaks are strongly supported by the $\beta_i(\epsilon)$ result. Conversely, this result suggests that even without an obligatory rule from angular momentum and parity considerations, β_i for a shake-up satellite will resemble that of its main line. We believe this approximate identity should hold for all satellites having the same term symbol as a main line. In Ar and Xe, Adam et al.[6] and Fahlman et al.[7] have observed that the $(^1D)md\ ^2S$ satellites have β_i like β_{ns}.

For the peak 6+7, consideration of binding energies alone gives an ambiguous identification. The β_i results suggest that one of the unresolved final states, $(^1D)3p\ ^2P^o$, is dominant. In the photon energy range of this experiment, the contribution from $(^1S)3s\ ^2S$ should be small because ionization of a 2p electron is much more probable than of a 2s electron. Wuilleumier and Krause[4] measured the angular distribution of peak 7 at photon energies of 132.3 and 151.4 eV. Obtaining a β_i value the same as β_{2p} within error, they estimated the maximum admixture of $(^1S)3s\ ^2S$ to be 25 percent. Using a similar assumption, namely:

$$\beta_7(\epsilon) = C_{3s}\ \beta_{2s}(\epsilon) + C_{3p}\ \beta_{2p}(\epsilon), \qquad (2)$$

and using $\beta_{2s}=2$ and the literature values for $\beta_{2p}(\epsilon)$,[11,15] we estimate the contribution of $(^1S)3s\ ^2S$, C_{3s} to be 10 ± 10 percent of satellite 7 in the low ϵ range.

The energy dependence of β_i for satellites 3 and 11 are quite different from either $\beta_{2s}(\epsilon)$ or $\beta_{2p}(\epsilon)$. Satellite 11 is associated with a single final state of symmetry ^2D, so that the satellite-producing mechanism is not final ionic-state configuration interaction (FISCI). A similar situation exists for helium in the photoelectron channel leading to $He^+(2p)$, for which β_i is quite different from that of the He 1s main line.[5]

For satellite 3 several final states are involved. As discussed earlier, the binding energy and broad width of this peak imply both a major contribution from the $(^1D)3d$ final states and the possible presence of additional components. Because β for this line is roughly constant, lying midway between $\beta(^2S) = 2$ and $\beta(^2P) = -1$, its intensity may be attributed to an approximately equal admixture of $(^1D)3d\ ^2P$ and ^2S final states. The slightly rising slope observed may then be due to a small admixture of $^2P^o$ states. A conclusive decomposition of satellite 3 would require a known β_i for the $(^1D)3d\ ^2D$ final state.

V. Partial Cross Sections

The primary data, intensity branching ratios between the satellite and the 2s line are shown in Table II. In Fig. 4 each measured ratio has been multiplied by the appropriate literature value

of σ_{2s},[11] yielding the satellite cross section, σ_i. To introduce the ϵ dependence in the shake model, Smid and Hansen[17] have included the variation of the main-line dipole matrix elements, e.g. $\langle \epsilon d|\vec{r}|2p\rangle$. This reasoning suggests that the satellite σ_i should resemble σ_{2p} at the same kinetic energy, where the continuum wavefunctions $\langle \epsilon d|$ will be most alike.

Several observations can be made from Fig. 4. All the satellites have $\sigma_i(\epsilon)$ varying similarly to $\sigma_{2p}(\epsilon)$, but except perhaps for satellite 3, the agreement is not exact. For example, $\sigma_i(\epsilon)$ for the satellite peak 6+7 exhibits a deviation that demonstrates a breakdown of the shake theory in the low-ϵ region. Ironically, $\sigma_i(\epsilon)$ of satellite 3 shows very close agreement with $\sigma_{2p}(\epsilon)$. This similarity must be regarded as fortuitous because the $\beta_i(\epsilon)$ data for this satellite (Fig. 3) disagree strongly with $\beta_{2p}(\epsilon)$. In addition, Fig. 4 shows that the various satellite $\sigma_i(\epsilon)$ curves differ, even for those three satellite peaks (4, 6+7, and 10) in which the $\beta_i(\epsilon)$ data track $\beta_{2p}(\epsilon)$. We conclude that near-threshold satellite intensities have complicated origins and cannot be simply predicted from main-line curves. Finally, the satellites $\sigma_i(\epsilon)$ do not display a tendency to approach zero at threshold. This final observation, along with the result that the $\sigma_i(\epsilon)$ curves are different, stand in conflict with the models of Stöhr et al.[18] and Thomas,[19] developed for core-level satellites.[20]

It is of interest to compare our near-threshold satellite intensities with previous work. In Table III our intensities at

ϵ = 10 eV and 40 eV are given as branching ratios relative to the 2p main line. Also listed are the measurements at 130 to 150 eV photon energy given by Wuilleumier and Krause,[4] and predicted values from the shake-theory calculation of Dyall and Larkins.[3] The literature values for both σ_{2s} and σ_{2p} were used to convert our data to the (satellite)/(2p) branching ratio. The precise values of Wuilleumier and Krause are in doubt because of an uncertainty in the normalization given by their Table V.[21] Nevertheless, their results indicate that the sudden-limit intensities of the individual satellites have not been reached at the highest photon energies of our experiment.

The qualitative agreement between the calculated and experimental intensities confirms that Dyall and Larkins' model includes the most important effects. Thus for the neon valence satellites, it appears that the relaxation which accompanies the formation of the hole and correlation in the final ionic state are important mechanisms. In this somewhat artificial division, we consider the change from the atomic to the ionic one electron orbitals separately from the multi-configurational description of the ionic state. These mechanisms may explain the populations of $^2P^o$ and ^2S final states, measured to be about 64 and 11 percent of all the satellite intensity, respectively. On the other hand, either initial state (ISCI) or continuum state configuration interaction (CSCI) must be invoked to explain the presence of the ^2D and ^2P satellites, about 25 percent of the satellite spectrum. By comparison, the intensity variation of satellite 11, $(^1D)3s\ ^2D$, is quite different from that of the He^+ 2p

satellite in the helium photoelectron spectrum, which is produced mainly by the CSCI process. The He 2p to 1s branching ratio decreases monotonically with increasing energy.[5] Thus the main contribution to satellite 11 may well be initial state configuration interaction. For the 5p satellites in the xenon spectrum, Hansen and Perssen[22] have suggested that initial state correlation plays the main role.

Satellite intensity data over a wider energy range is desirable, but the available data are very limited. For the single case of satellites 6+7 it is possible to extend the data range to $\epsilon \sim 1.5$ keV, by combining our results with intensities given by Wuilleumier and Krause.[4] The combined data are shown in Fig. 5, plotted against a logarithmic kinetic energy scale. Unfortunately, these data must be interpreted with caution, because the high intensities observed at the three highest kinetic energies may not represent an enhancement of a single satellite process. At these energies, the 2s channel has become stronger than the 2p, and as a consequence the $(^1S)3s\ ^2S$ satellite may dominate over the $(^1D)3p\ ^2P^o$.

Also plotted in Fig. 5 is a curve representing a theoretical treatment of the satellite intensity variation from the adiabatic to sudden limits.[19] This model of Thomas is based on a specific "shake-up" mechanism during the creation of the hole state. The relative intensity ratio μ is given by

$$\mu = \mu_\infty \exp(-mr^2 E_o / 2\hbar^2 E_{ex}), \qquad (3)$$

where m is the electron mass, E_0 refers to the energy separation between the satellite and main-line final states, and E_{ex} is the excitation energy of the satellite electron above the main line threshold, i.e., $E_{ex} = E_0+\epsilon$. The adjustable parameters, μ_∞ and r, are the sudden-limit intensity ratio and an effective radius, respectively. For the curve shown in Fig. 5, both parameters were varied to achieve the best reasonable fit with the data (μ_∞ = 3.7 percent and r = 0.78Å); the highest energy points were excluded from the fit for the reason mentioned above.

With suitable adjustment, the model can be made to fit the data in Fig. 5. However, there are at least two reasons for caution in appraising this agreement. First, the model must be regarded with skepticism at low values of ϵ, because it does not explicitly require energy conservation [$\mu(\epsilon<0) > 0$]. Second, the low-energy behavior of satellites 6+7 cannot be regarded as typical. For comparison, the nearly constant intensity ratio for satellite 10 is included in Fig. 5. Satellite intensity ratios which decrease as kinetic energy increases have been observed in He[5] and Ar.[6] Eqn. (3) cannot provide a universal curve for this complex variety of energy-dependent satellite intensities. We conclude that the results in Fig. 5 give an intriguing but not yet definitive view of the energy variation of satellite intensities.

VI. Conclusion

We have described the measurement of the binding energies,

asymmetry parameters, and partial cross sections for the neon valence satellites. Observing the satellite spectrum at low photon energies, certain types of final state configurations are found to be more important than others. Of the final states with unambiguous parentage, ^2S and $^2P^o$, the $^2P^o$ states receive greater intensity, which suggests that the satellites mainly "borrow" intensity from the 2p main line. In addition, the excited orbital is usually in the n=3 shell. For the $^2P^o$ satellites, $\beta_i(\epsilon)$ follows $\beta_{2p}(\epsilon)$ closely. Therefore, as a general rule, a satellite having the same ^{2S+1}L as the main line also should have a $\beta_i(\epsilon)$ which tracks the $\beta(\epsilon)$ of the main line. Other satellites may have quite different $\beta_i(\epsilon)$ dependence, as seen from the $\beta(\epsilon)$ results. All σ_i approximately imitate σ_{2p} as a function of kinetic energy. The observed deviations of $\sigma_i(\epsilon)$ from $\sigma_{2p}(\epsilon)$ remain puzzling. These differences do suggest that the sudden limit has not been reached by $\epsilon \sim 40$ eV ($\epsilon/E_o \sim 1.2$). Comparison of the experiments with the calculation of Dyall and Larkins[3] confirms the importance of relaxation and FISCI. However, to explain the presence of ^2D and ^2P satellites, some other mechanism must contribute, such as initial state correlation. The neon valence satellites represent a problem which has been partly solved. Two very useful contributions would be: (1) a measurement of β_i at high energy, e.g. $h\nu = 1$ keV, in order to determine the role of the 2s satellites, (2) a calculation of σ_i which includes ISCI.

Acknowledgements

We are grateful to M.Y. Adam for providing her unpublished results. This work was supported by the Director, Office of Energy Research, Office of Basic Energy Sciences, Chemical Sciences Division of the U.S. Department of Energy under Contract No. DE-AC03-76SF00098. It was performed at the Stanford Synchrotron Radiation Laboratory, which is supported by the Department of Energy, Office of Basic Energy Sciences and the National Science Foundation, Division of Materials Research. One of us (H.G.K.) acknowledges support by a Wigner fellowship, and one of us (U.B.) acknowledges support from the Deutsche Forschungsgemeinschaft (DFG).

References

1. T. Åberg, Phys. Rev. 156, 35 (1967).
2. K.G. Dyall and F.P. Larkins, J. Phys. B 15, 203 (1982) and references therein.
3. K.G. Dyall and F.P. Larkins, J. Phys. B 15, 219 (1982).
4. F. Wuilleumier and M.O. Krause, Phys. Rev. A 10, 242 (1974).
5. D.W. Lindle, T.A. Ferrett, U. Becker, P.H. Kobrin, C.M. Truesdale, H.G. Kerkhoff and D.A. Shirley, to be published; F. Wuilleumier, J. de Physique C2, 347 (1982) and references therein.
6. M.Y. Adam, P. Morin and G. Wendin, to be published.
7. A. Fahlman, M.O. Krause and T.A. Carlson, J. Phys. B 17, L217 (1984); A. Fahlman, M.O. Krause, T.A. Carlson and A. Svensson, Phys. Rev. A 30, 812 (1984).
8. M.G. White, R.A. Rosenberg, G. Gabor, E.D. Poliakoff, G. Thornton, S.H. Southworth and D.A. Shirley, Rev. Sci. Instr. 50, 1268 (1979).
9. S.H. Southworth, C.M. Truesdale, P.H. Kobrin, D.W. Lindle, W.D. Brewer and D.A. Shirley, J. Chem. Phys. 76, 143 (1982); S. Southworth, U. Becker, C.M. Truesdale, P.H. Kobrin, D.W. Lindle, S. Owaki, and D.A. Shirley, Phys. Rev. A 28, 261 (1983).
10. C.N. Yang, Phys. Rev. 74, 764 (1948).
11. F. Wuilleumier and M.O. Krause, J. Electron Spectrosc. Relat. Phenom. 15, 15 (1979).
12. W. Perssen, Phys. Scr. 3, 133 (1971).
13. C.E. Moore, Atomic Energy Levels, NBS Circular 467 (U.S. GPO,

Washington, D.C., 1949), Vol. 1.

14. S.T. Manson and A.F. Starace, Rev. Mod. Phys. 54, 389 (1982).

15. M.Y. Adam, private communication.

16. G.V. Marr and J.B. West, Atom. Data 18, 497 (1976).

17. H. Smid and J.E. Hansen, Phys. Rev. Lett. 52, 2138 (1984).

18. J. Stöhr, R. Jaeger and J.J. Rehr, Phys. Rev. Lett. 51, 821 (1983).

19. T.D. Thomas, Phys. Rev. Lett. 52, 417 (1984).

20. While the function provided by Thomas does not go to zero at the satellite threshold, he suggests that the intensity should vanish because of the shrinking of phase space.

21. In Table V of Ref. 4, the columns labelled Peak 7(i) and Total provide normalizations which differ by 30 percent. Manfred Krause has suggested that the Peak 7(i) scaling should be correct.

22. J.E. Hansen and W. Perssen, Phys. Rev. A 30, 1565 (1984).

Table I. The neon valence satellite binding energies from the present work together with the assignments of Dyall and Larkins[3] and with the energies of Perssen[12] from emission spectroscopy. All the satellite final states include a $1s^2 2s^2 2p^4$ core.

Peak	Binding Energy (eV)	Assignment	Optical Energy (eV)
1	62.27(10)	$(^1D)5p\ ^2P^o$	
		$(^1D)4d\ ^2S$	
2	61.02(10)	$(^1D)4p\ ^2P^o$	60.96
3	59.56(7)	$(^3P)5p\ ^2P^o$	59.83
		$(^1D)3d\ ^2D$	59.54
		$(^1D)3d\ ^2S$	59.51
		$(^1D)3d\ ^2P$	59.46
		$(^1S)3p\ ^2P^o$	59.40
4	58.06(6)	$(^3P)4p\ ^2P^o$	58.01
6	56.41(5)	$(^3P)3d\ ^2P$	56.48
		$(^3P)3d\ ^2D$	56.33
7	55.85(4)	$(^1S)3s\ ^2S$	55.87
		$(^1D)3p\ ^2P^o$	55.80

Table I. Continued.

Peak	Binding Energy (eV)	Assignment	Optical Energy (eV)
10	53.10(4)	$(^3P)3p\ ^2P^o$	53.06
11	52.13(3)	$(^1D)3s\ ^2D$	52.12
2s			48.48
2p			21.57

Table II. The asymmetry parameter values and branching ratios with respect to the 2s main line. The error in the last digits is noted in parentheses.

Peak	K.E. (eV)	Asymmetry Parameter (β)	Branching Ratio (%)	Peak	K.E. (eV)	Asymmetry Parameter (β)	Branching Ratio (%)
3	3.3	-	11.9 (33)	4	3.6	-0.42 (10)	4.5 (8)
	4.4	0.41 (23)	11.0 (16)		4.7	-0.06 (21)	3.2 (5)
	7.1	0.55 (5)	12.6 (8)		5.9	0.19 (15)	3.4 (7)
	10.7	0.56 (11)	12.4 (3)		8.6	0.43 (22)	3.4 (1)
	12.8	0.52 (6)	13.0 (4)		12.2	0.74 (42)	3.1 (4)
	15.8	0.55 (12)	12.0 (18)		14.3	0.81 (15)	3.3 (2)
	20.9	0.52 (5)	12.0 (3)		17.3	0.95 (24)	3.2 (4)
	25.9	0.44 (12)	11.3 (12)		22.4	1.14 (39)	3.4 (5)
	31.0	0.86 (7)	9.3 (6)		27.4	1.06 (37)	2.9 (8)
	36.1	0.57 (24)	9.5 (15)		32.5	1.47 (27)	2.6 (6)
	40.1	0.76 (15)	8.3 (7)		37.6	1.43 (44)	3.1 (7)
					41.6	0.91 (26)	3.4 (4)
6	4.7	-0.04 (4)	19.1 (6)	10	3.2	-	12.7 (33)
+	5.9	0.14 (7)	20.5 (13)		4.0	-	11.0 (6)
7	6.9	0.17 (11)	20.2 (9)		6.0	-0.20 (2)	12.5 (5)
	8.0	0.31 (10)	22.2 (11)		7.2	-0.01 (14)	9.6 (3)
	10.7	0.35 (7)	22.9 (8)		8.8	0.13 (34)	9.6 (9)
	14.3	0.71 (14)	22.6 (18)		9.7	0.17 (3)	10.1 (3)
	16.4	0.70 (4)	23.9 (5)		10.9	0.17 (8)	10.0 (4)

Table II. Continued.

Peak	K.E. (eV)	Asymmetry Parameter (β)	Branching Ratio (%)	Peak	K.E. (eV)	Asymmetry Parameter (β)	Branching Ratio (%)
6	19.5	0.87 (20)	23.7 (12)	10	13.6	0.35 (13)	9.2 (5)
+	24.5	1.04 (11)	24.7 (4)		17.2	0.68 (20)	7.8 (2)
7	29.6	1.10 (9)	24.2 (7)		19.3	0.68 (6)	7.7 (2)
	34.6	1.11 (8)	24.4 (9)		22.3	0.70 (7)	7.4 (5)
	39.7	1.26 (7)	23.7 (5)		27.4	0.81 (12)	7.0 (5)
	43.8	1.27 (10)	23.3 (9)		32.5	0.76 (25)	6.2 (6)
					37.5	0.97 (29)	5.5 (6)
					42.6	1.23 (16)	5.1 (3)
11	3.3	-	13.1 (23)				
	4.1	1.24 (18)	7.6 (7)				
	5.0	1.68 (25)	7.0 (12)				
	7.0	0.51 (4)	8.6 (3)				
	8.2	0.18 (15)	7.1 (15)				
	9.7	-0.01 (10)	6.4 (3)				
	10.7	-0.12 (5)	6.8 (6)				
	11.9	-0.22 (7)	6.6 (2)				
	14.6	-0.20 (6)	6.2 (4)				
	18.2	-0.27 (7)	6.9 (6)				
	20.3	-	7.2 (2)				
	23.3	-0.34 (13)	6.6 (6)				
	28.4	0.16 (25)	6.8 (5)				
	33.4	0.27 (13)	6.1 (5)				
	38.5	-	5.2 (12)				

Table III. Relative satellite intensities as a ratio with the 2p line. The results of this work are compared with the higher energy measurement of Wuilleumier and Krause[4] and with the sudden limit calculation of Dyall and Larkins.[3]

Satellite Peak No.	10 eV Kinetic Energy	40 eV Kinetic Energy	Experiment at 130-150 eV Photon Energy[a]	Calculation[b]
3	0.81	0.85	0.54	0.41-0.61
4	0.20	0.33	0.49	0.36
6+7	1.34	2.33	2.55	1.13-1.24
10	0.52	0.51	0.68	0.28
11	0.32	0.48	0.35	-
Sum	3.19	4.50	4.61	2.18-2.49

[a]Wuilleumier and Krause's reported intensities for satellites 5, 8, 9, and 12 have been added to their neighbor satellite peak.

[b]The calculated contributions from ^2S states have been multiplied by the ratio σ_{2s}/σ_{2p} at 55-150 eV photon energy.[10]

Figure Captions

Fig. 1. A photoelectron spectrum of Ne taken at 64.1 eV photon energy with the 0° analyzer. The solid line represents a least-squares fit. The prompt peak results from light scattered by the gas sample onto the detector. The satellite peak labels follow the notation of Wuilleumier and Krause.[4] Though not shown, the 2p peak occurs at 42.5 eV kinetic energy.

Fig. 2. The satellite peak widths from spectra with low analyzer retarding voltage.

Fig. 3. The asymmetry parameter as a function of the satellite kinetic energy is shown with each satellite in a separate panel. The solid lines represent β_{2p} shifted to the equivalent kinetic energy.[15] The open squares display β_i values obtained by Adam.[15]

Fig. 4. The partial cross section as a function of the satellite kinetic energy is shown. The solid lines represent σ_{2p} divided by a large integer and shifted to be at the same kinetic energy as the satellite.[11,16]

Fig. 5. The branching ratio of satellite peaks 6+7 and 10 with respect to the 2p main line is presented. The circles show our results (filled) and those of Wuilleumier and Krause[4] (open) for satellites 6+7, and the squares show the present results for satellite 10. The solid line represents the model function of Thomas[19] evaluated with μ_∞=3.7 percent and r=0.78Å.

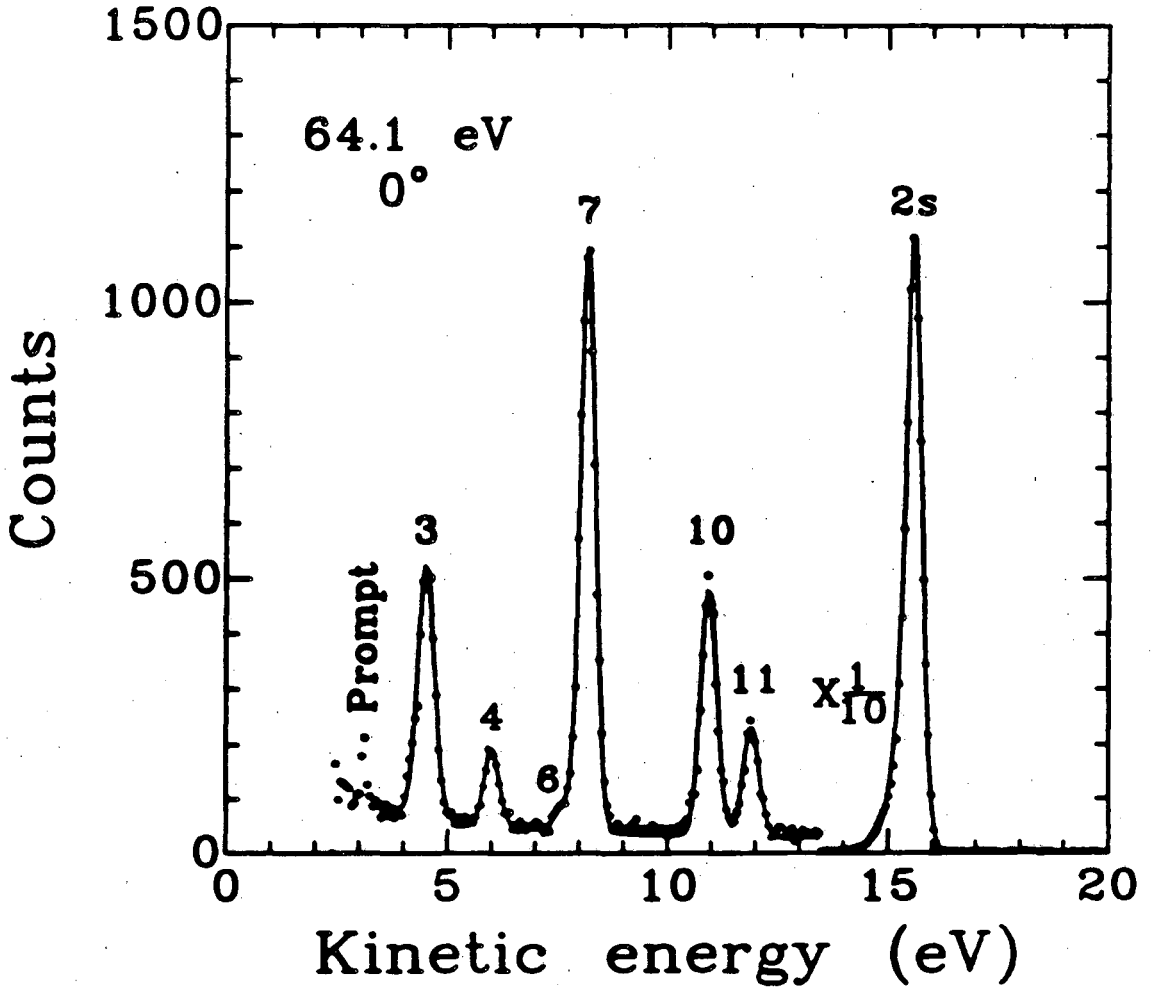

XBL 845-1986A

Figure 1

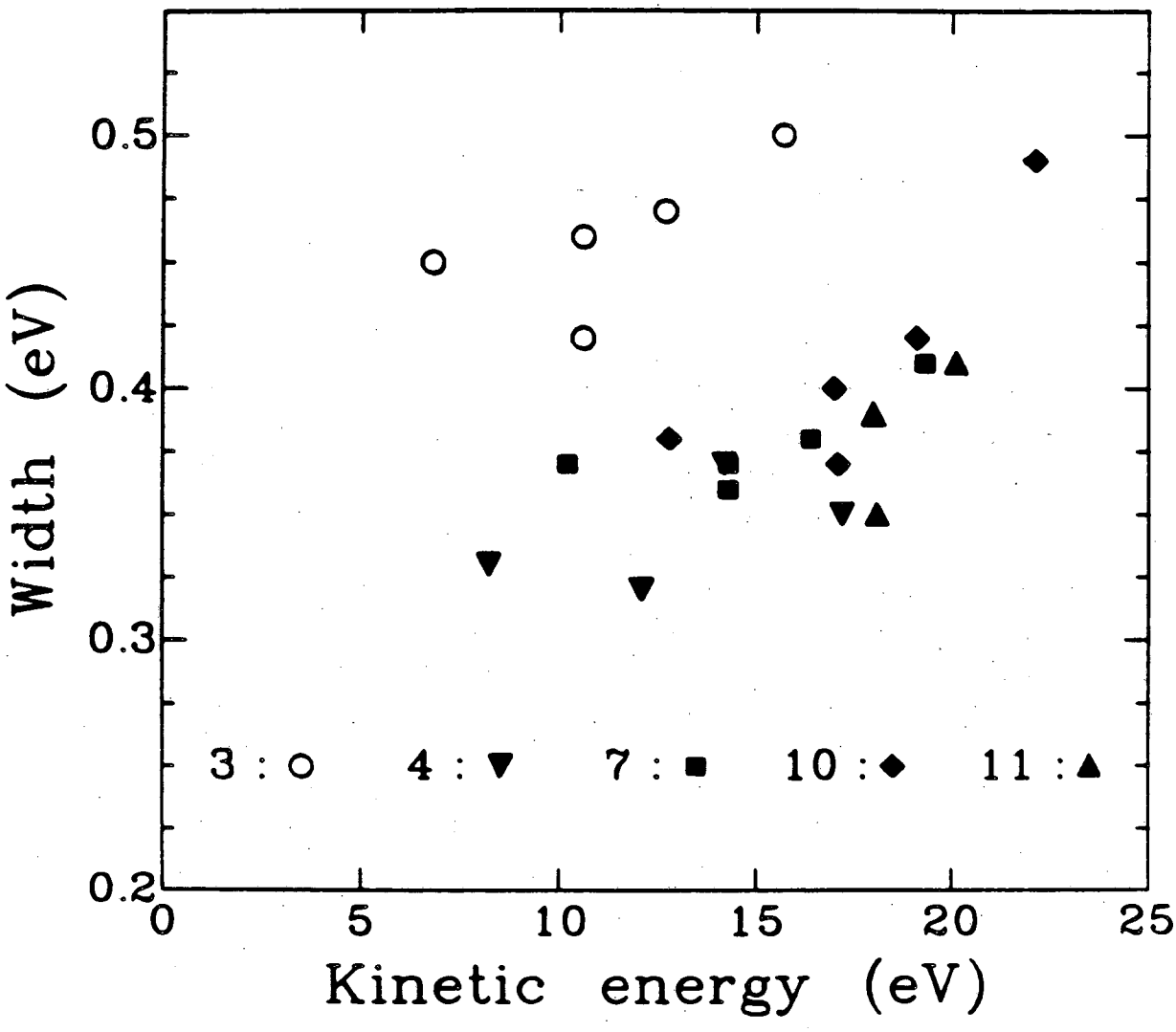

XBL 8410-4569

Figure 2

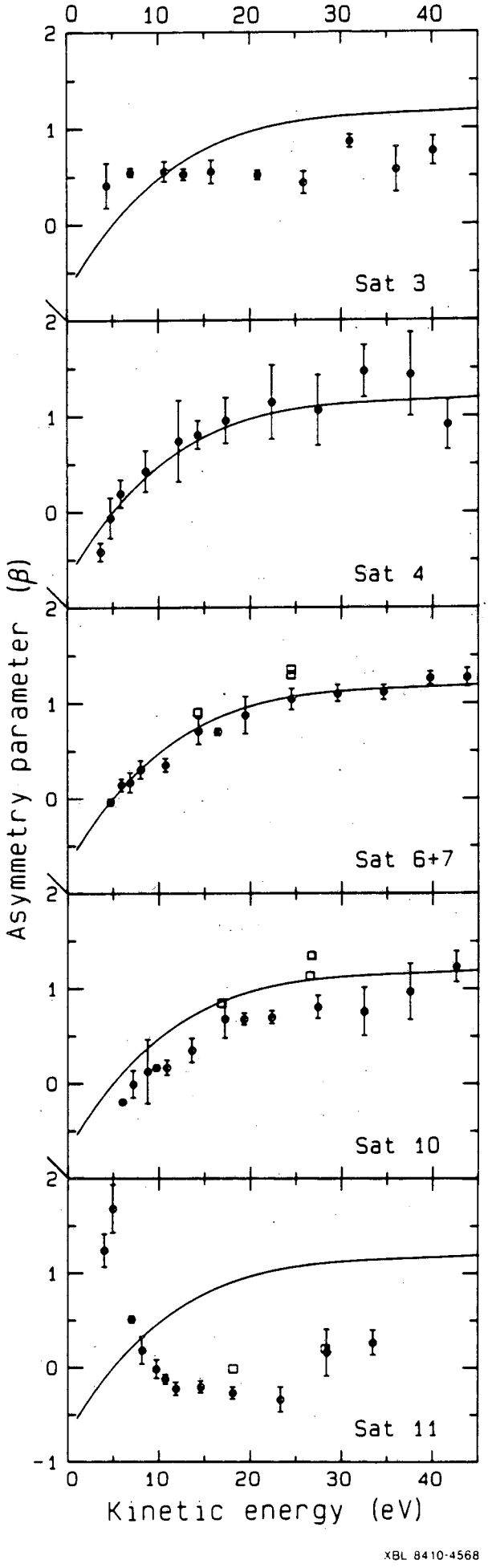
Asymmetry parameter (β)
Kinetic energy (eV)
Sat 3
Sat 4
Sat 6+7
Sat 10
Sat 11
XBL 8410-4568

Figure 3

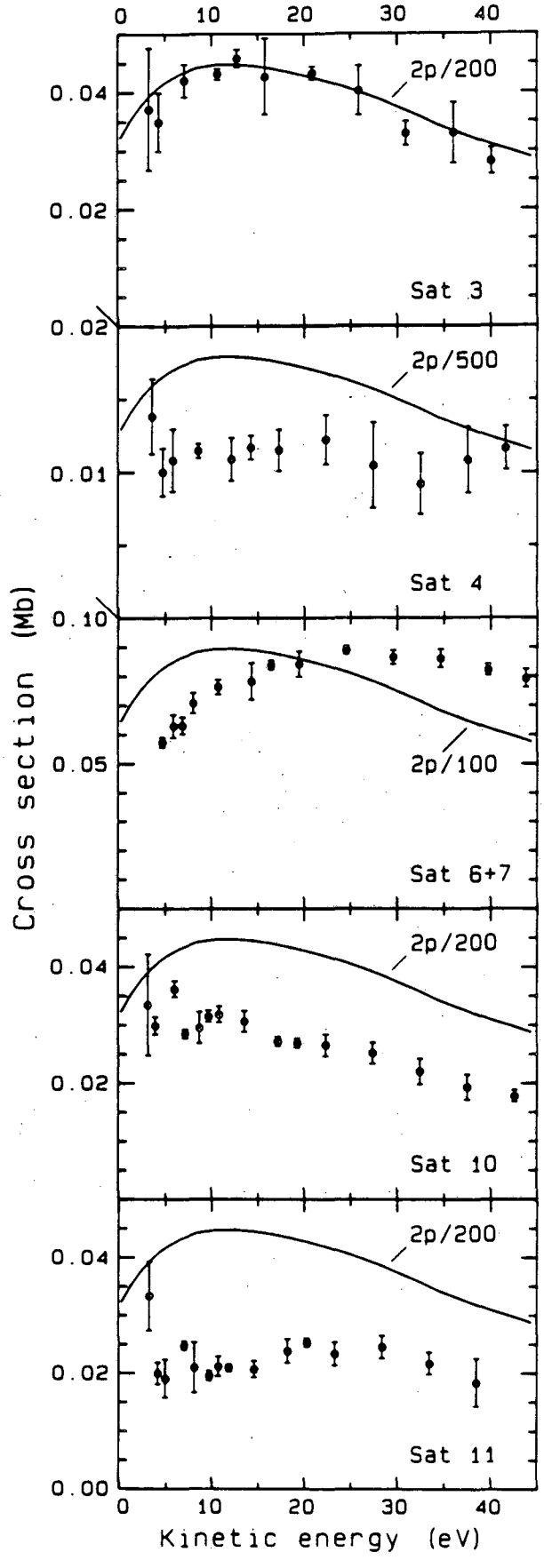
0
10
20
30
40
2p/200
0.04
0.02
Sat 3
0.02
2p/500
0.01
Sat 4
0.10
2p/100
0.05
Sat 6+7
2p/200
0.04
0.02
Sat 10
2p/200
0.04
0.02
Sat 11
0.00
0
10
20
30
40
Cross section (Mb)
Kinetic energy (eV)
XBL 8410-4567

Figure 4

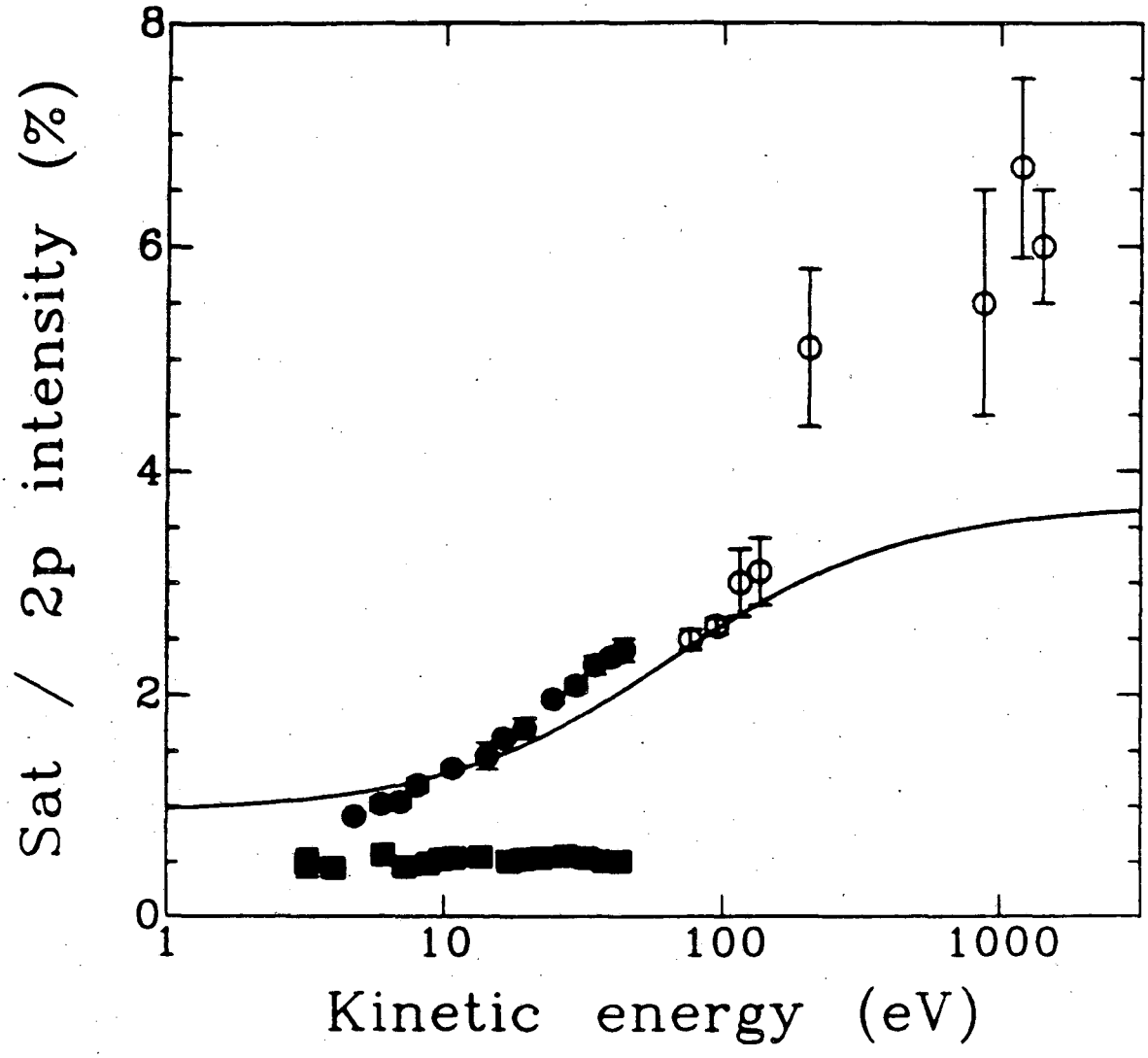
Sat / 2p intensity (%)
0
2
4
6
8
1
10
100
1000
Kinetic energy (eV)
XBL 8410-4570

Figure 5

TECHNICAL INFORMATION DEPARTMENT
LAWRENCE BERKELEY LABORATORY
UNIVERSITY OF CALIFORNIA
BERKELEY, CALIFORNIA 94720